J|A|C|S COMMUNICATIONS

Published on Web 01/12/2009

Porous Nanoparticle Supported Lipid Bilayers (Protocells) as Delivery Vehicles

Juewen Liu,[†] Alison Stace-Naughton,[†] Xingmao Jiang,[†] and C. Jeffrey Brinker*[,†,‡,§]

Center for Micro-Engineered Materials and Departments of Chemical and Nuclear Engineering and Molecular Genetics and Microbiology, University of New Mexico, and Sandia National Laboratories, Albuquerque, New Mexico 87106

Received October 10, 2008; E-mail: cjbrink@sandia.gov

A major challenge in nanomedicine is to engineer nanostructures and materials that can efficiently encapsulate drugs at high concentration, cross the cell membrane, and controllably release the cargo at the target site over a prescribed period of time.[1] Recently, inorganic nanoparticles have emerged as a new generation of drug/therapy delivery vehicles in nanomedicine.[2,3] Mesoporous silica nanoparticles are particularly attractive because of their biocompatibility and precisely defined nanoporosity.[4−7] With uniform, tunable pore diameters, ranging from ∼2 to 5 nm and surfaces areas of 700−1300 m^2/g, drugs and other components can be loaded by adsorption or capillary filling, and the release profiles adjusted by the combination of pore size and pore surface chemistry.[8] Very recently, elegant gating methods, employing coumarin,[9] azobenzene,[10,11] rotaxane,[12] polymers,[13,14] or nanoparticles,[15,16] have been established to seal the cargo within the particle and allow its triggered release according to an optical or electrochemical stimulus. Here we describe a synergistic system where liposome fusion on a mesoporous silica particle core simultaneously loads and seals the cargo, creating a "protocell" construct useful for delivery across the cell membrane (Figure 1B). We observe that fusion of a positively charged liposome on a negatively charged mesoporous silica core serves to load the core with a negatively charged dye (excluded from the mesopores without lipid) to concentrations that can exceed 100× those in solution. Sealed within the protocell, this membrane impermeable dye can be transported across the cell membrane and slowly released within the cell. Compared to other nanoparticle delivery systems, the protocell is simple and takes advantage of the low toxicity and immunogenicity of liposomes along with their ability to be PEGylated or conjugated to extend circulation time and effect targeting. Compared to liposomes, however, the protocell is more stable and takes advantage of the mesoporous core to control both loading and release. As noted in many other relevant papers the mesoporous core can be used additionally to deliver DNA, hydrophobic anticancer drugs, and proteins.[17−19]

Mesoporous silica particle "cores" were prepared by the surfactant templated aerosol-assisted self-assembly method developed in our group.[20] After removal of surfactant templates, we obtain hydrophilic nanoparticles characterized by a uniform, ordered, and connected mesoporosity with a specific surface area of 935 m^2/g. A representative TEM image of the mesoporous particles is shown in Figure 1A along with a dynamic light scattering histogram, indicating the average particle size to be ∼100 nm. Liposomes were prepared by extrusion of hydrated lipid films through a filter with a pore size of 100 nm using standard protocols and fused with the cores by pipet mixing. Such supported bilayers have been studied extensively as model systems for cell membranes,[21,22] whereas their applications in drug delivery have yet to be explored.

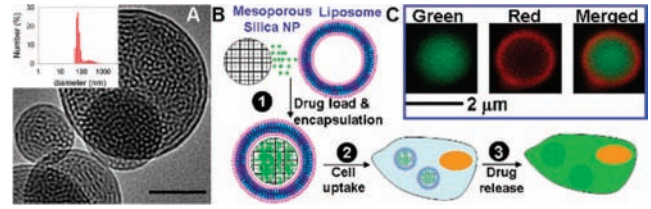

Figure 1. (A) Representative TEM image of mesoporous silica nanoparticle cores. Scale bar = 50 nm. Inset: dynamic light scattering histogram. (B) Simultaneous loading and encapsulation of drugs through liposome fusion on mesoporous silica nanoparticles (1); cellular uptake of loaded protocells (2); and release within cells (3). (C) Confocal fluorescence images of the FITC-labeled mesoporous core, Texas Red-labeled lipid, and merged image confirming the postulated construct.

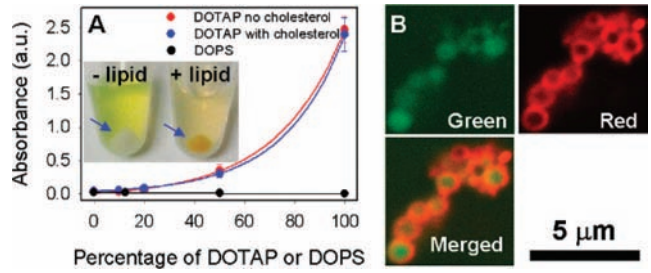

Figure 2. (A) Calcein incorporation in mesoporous silica cores after fusion with DOPC/DOTAP or DOPC/DOPS liposomes. Inset: optical image of centrifuged mesoporous silica cores (indicated by the arrows) after incubation with 250 μM calcein solutions with and without DOTAP liposomes. (B) Confocal fluorescence images of calcein loaded protocells formed by fusion of Texas Red-labeled DOTAP liposomes. Green channel, calcein; red channel, Texas Red; merged = red + green.

Although the sizes of most silica nanoparticles were below the optical resolution of fluorescence microscopy, a small fraction of large nanoparticles were obtained by sedimentation. Figure 1C shows a confocal image of a protocell, where the core was labeled with FITC and the lipid was labeled with Texas Red. A green core and a red shell are clearly observed, confirming liposome fusion on the mesoporous core.

To demonstrate the concept of loading and sealing the silica core through liposome fusion, calcein was chosen as a model drug/probe, because it is membrane impermeable and fluorescent. Incubated with the silica core in the absence of liposomes, the negatively charged dye does not enter the internal mesoporosity due to electrostatic considerations, and the silica cores concentrated at the bottom of the tube by centrifugation are colorless (Figure 2A, inset). Calcein uptake accompanying liposome fusion was determined by incubation of

[†] Center for Micro-Engineered Materials, University of New Mexico.
[‡] Departments of Chemical and Nuclear Engineering and Molecular Genetics and Microbiology, University of New Mexico.
[§] Sandia National Laboratories.

10.1021/ja808018y CCC: $40.75

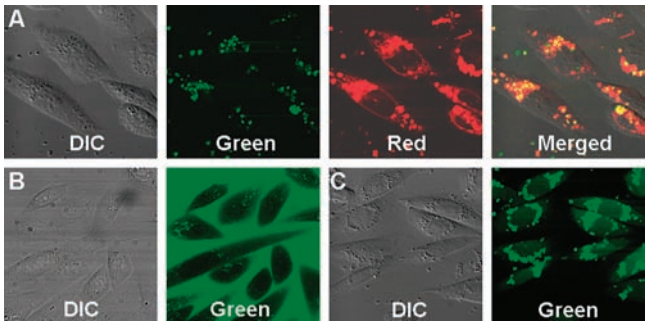

Figure 3. Confocal fluorescence images of protocells incubated with CHO cells. (A) FITC-labeled core and Texas Red-labeled DOTAP shell. (B) CHO incubated with free calcein in media. (C) CHO incubated with calcein encapsulated in supported DOTAP bilayers.

mesoporous cores in a calcein solution to which liposomes were added. After incubation for 10 min, unincorporated dye was removed by multiple rounds of centrifugation, supernatant removal, and washing until no calcein was detectable in the supernatant. The encapsulated calcein was quantified by adding a surfactant (SDS) to release the dye into solution and measuring its absorbance at 500 nm. Figure 2A shows absorbance measurements as a function of lipid composition conducted with liposomes composed of the zwitterionic lipid 1,2-dioleoyl-*sn*-glycero-3-phosphocholine (DOPC) plus varying percentages of the negatively charged lipid 1,2-dioleoyl-*sn*-glycero-3-phosphoserine (DOPS) or positively charged lipid 1,2-dioleoyl-3-trimethylammonium-propane (DOTAP). We observe essentially no calcein loading of the mesoporous core fused with DOPC or liposomes containing the negatively charged DOPS. This is consistent with the fact that, without liposomes, calcein does not enter the pores and, for the limiting case of 100% DOPS, there is no liposome fusion with the core (see Supporting Information), emphasizing the role of electrostatic interactions in loading and fusion. In contrast, for protocells formed by fusion of positively charged DOTAP, we observe an exponential increase in calcein loading with the percentage of DOTAP (Figure 2A). These results reveal a synergistic system where loading of the negatively charged drug model occurs only by fusion of the positively charged liposome with the negatively charged core. Loading is controlled by the lipid composition, independently of cholesterol, and as evident in the Figure 2A inset, the core calcein concentration can exceed greatly that in solution (enrichment factor $\sim$110$\times$ for the 100% DOTAP composition; see Supporting Information). Confocal imaging (Figure 2B) of representative sub-μm diameter protocells reveals the calcein loading to occur throughout the volume of the core. For cores exceeding several micrometers in diameter, loading was confined to a $\sim$0.5-μm thick shell at the core surface. Calcein release profiles determined in buffer for the DOTAP protocell showed 90% release in 18 days (see Supporting Information). It is important to note that the loading and release for the protocell construct are qualitatively different than those of conventional liposomes, where the cargo concentration is approximately that of the solution in which liposomes are formed (no enrichment) and the release is practically instantaneous.

To study protocell entry into mammalian cells and the feasibility of their use for drug delivery, protocells prepared by fusion of Texas Red-labeled DOTAP liposomes on FITC-labeled mesoporous silica cores (as in Figure 1C, but sub-μm in diameter) were incubated with Chinese hamster ovary cells (CHO) at 37 °C for 4 h. The cells were then washed extensively and imaged via confocal fluorescence microscopy. As observed in Figure 3A, most cells exhibited overlapped green and red fluorescence, suggesting that the core and lipid bilayer were incorporated concurrently as expected for endocytosis. (Additional "smeared-out" red emission indicates some loss of liposome from the core through either lipid exchange or membrane fusion.) To test delivery from the synergistically loaded and sealed protocells, calcein loaded protocells were prepared from DOTAP and incubated with cells as in Figure 1B. Green fluorescence was observed throughout the cells (Figure 3C). In contrast, when membrane impermeable, free calcein was incubated with CHO cells, no cellular uptake was observed (Figure 3B). From a pH-dependent study performed in vitro, we determined calcein release to be much faster at lower pH compared to that at pH 8 (see Supporting Information). Because the loaded protocells most likely reside in endosomal compartments with a localized pH of $\sim$5.0, release should be facilitated inside the cells as evident from dimmer fluorescence adjoining brighter regions within cells (Figure 3C), which we postulate to be calcein release into the cytosol.

In summary, we have shown that fusion of a positively charged liposome with a negatively charged mesoporous silica core synergistically loads and seals a negatively charged cargo within the core. Adjustment of the liposome composition/charge allows control of the cargo content, whose concentration can greatly exceed that of the surrounding solution. The protocells can be internalized by mammalian cells and, due to enhanced release at lower pH, can deliver their contents within the cell. Compared to some other nanoparticle systems, protocells provide a simple construct for loading, sealing, delivering, and releasing and should serve as a useful vector in nanomedicine.

Acknowledgment. This work is funded by the National Institutes of Health through the NIH Roadmap for Medical Research, DOE Office of Science, and Air Force Office of Scientific Research.

Supporting Information Available: Methods. This material is available free of charge via the Internet at http://pubs.acs.org.

References

(1) Langer, R. *Nature* **1998**, *392*, 5–10.
(2) Sokolova, V.; Epple, M. *Angew. Chem., Int. Ed.* **2008**, *47*, 1382–1395.
(3) Rosi, N. L.; Mirkin, C. A. *Chem. Rev.* **2005**, *105*, 1547–1562.
(4) Vallet-Regi, M.; Balas, F.; Arcos, D. *Angew. Chem., Int. Ed.* **2007**, *46*, 7548–7558.
(5) Slowing, I. I.; Trewyn, B. G.; Giri, S.; Lin, V. S. Y. *Adv. Funct. Mater.* **2007**, *17*, 1225–1236.
(6) Julian-Lopez, B.; Boissiere, C.; Chaneac, C.; Grosso, D.; Vasseur, S.; Miraux, S.; Duguet, E.; Sanchez, C. *J. Mater. Chem.* **2007**, *17*, 1563–1569.
(7) Schlossbauer, A.; Schaffert, D.; Kecht, J.; Wagner, E.; Bein, T. *J. Am. Chem. Soc.* **2008**, *130*, 12558–12559.
(8) Jiang, X. M.; Brinker, C. J. *J. Am. Chem. Soc.* **2006**, *128*, 4512–4513.
(9) Mal, N. K.; Fujiwara, M.; Tanaka, Y. *Nature* **2003**, *421*, 350–353.
(10) Liu, N. G.; Dunphy, D. R.; Atanassov, P.; Bunge, S. D.; Chen, Z.; Lopez, G. P.; Boyle, T. J.; Brinker, C. J. *Nano Lett.* **2004**, *4*, 551–554.
(11) Angelos, S.; Choi, E.; Vogtle, F.; De Cola, L.; Zink, J. I. *J. Phys. Chem. C* **2007**, *111*, 6589–6592.
(12) Nguyen, T. D.; Tseng, H. R.; Celestre, P. C.; Flood, A. H.; Liu, Y.; Stoddart, J. F.; Zink, J. I. *Proc. Natl. Acad. Sci. U.S.A.* **2005**, *102*, 10029–10034.
(13) Wang, Y. J.; Caruso, F. *Chem. Commum.* **2004**, 1528–1529.
(14) Radu, D. R.; Lai, C. Y.; Wiench, J. W.; Pruski, M.; Lin, V. S. Y. *J. Am. Chem. Soc.* **2004**, *126*, 1640–1641.
(15) Lai, C. Y.; Trewyn, B. G.; Jeftinija, D. M.; Jeftinija, K.; Xu, S.; Jeftinija, S.; Lin, V. S. Y. *J. Am. Chem. Soc.* **2003**, *125*, 4451–4459.
(16) Giri, S.; Trewyn, B. G.; Stellmaker, M. P.; Lin, V. S. Y. *Angew. Chem., Int. Ed.* **2005**, *44*, 5038–5044.
(17) Torney, F.; Trewyn, B. G.; Lin, V. S. Y.; Wang, K. *Nat. Nanotechnol.* **2007**, *2*, 295–300.
(18) Slowing, I. I.; Trewyn, B. G.; Lin, V. S. Y. *J. Am. Chem. Soc.* **2007**, *129*, 8845–8849.
(19) Lu, J.; Liong, M.; Zink, J. I.; Tamanoi, F. *Small* **2007**, *3*, 1341–1346.
(20) Lu, Y. F.; Fan, H. Y.; Stump, A.; Ward, T. L.; Rieker, T.; Brinker, C. J. *Nature* **1999**, *398*, 223–226.
(21) Grakoui, A.; Bromley, S. K.; Sumen, C.; Davis, M. M.; Shaw, A. S.; Allen, P. M.; Dustin, M. L. *Science* **1999**, *285*, 221–227.
(22) Cornell, B. A.; BraachMaksvytis, V. L. B.; King, L. G.; Osman, P. D. J.; Raguse, B.; Wieczorek, L.; Pace, R. J. *Nature* **1997**, *387*, 580–583.

JA808018Y